



EFFECT OF ABSORBER DESIGN ON CONVECTIVE HEAT TRANSFER IN A FLAT PLATE SOLAR COLLECTOR: A CFD MODELING

E. Flihi^{a,†}, E. H. Sebbar^a, D. Achemlal^a, T. EL Rhafiki^a, M. Sriti^b, E. Chaabelasri^c

^aSidi Mohamed Ben Abdellah University, Polydisciplinary Faculty of Taza, Engineering Sciences Laboratory, BP.1223, Taza, Morocco

^bMoulay Ismail University, ENSAM Engineering School, Energy Department, Marjane 2, BP 15290, Al Mansour Meknes, Morocco

^cMohamed First University, Faculty of Sciences, PTPME Laboratory, BP 717, Oujda, Morocco

ABSTRACT

In this paper, we made a numerical simulation of convective heat transfer in a rectangular section pipe of an air flat plate solar collector using three forms of the absorber plate namely, simple shape, rectangular-shape, and half circle-shape. The flow is considered laminar and stationary, where the heat exchange between the absorber plate and the fluid takes place in useful area. The computer code in fluid dynamics, the fluent, is applied to integrate the governing equations on each control volume. A detailed description of the fluid flow and heat transfer in the rectangular channel was made. Several simulations were carried out in order to determine the influencing parameters allowing better performances of the collector and ensuring a good homogeneity of the temperature at the exit of the channel. The obtained results showed that the low mass flow rates of the air increase the average outlet temperature. Also, the use of the second configuration of the absorber (rectangular shape) increases the velocity of the air at the downstream of the channel and promotes more the thermal homogeneity at the outlet of the channel.

Keywords: Solar collector, working fluid, control volume, fluent, absorber.

1. INTRODUCTION

The increasing energy consumption requires serious attention, in this context, renewable energy is highly needed to support the global and national use of energy. One of the renewable energy is solar energy, which is eco-friendly, cheap, and easy to get especially in Morocco, which has one of the highest rates of solar insolation among other countries, about 3,000 hours per year of sunshine but up to 3,600 hours in the desert. Solar energy can be converted to useful thermal energy with solar collector that is essential device for any active solar air system. It is responsible for collecting solar radiation and converting it to heat which is transferred to the working fluid. The thermal energy obtained can be used for heating buildings, for the production of domestic hot water, or in various industrial processes, namely an indirect solar dryer.

Improving the performance of solar collectors consists of limiting heat loss between the absorber and the environment and increasing the quantity of energy absorbed with a judicious choice of the form and type of the absorber components. In this sense, several theoretical and experimental research works have been carried out on solar collectors to optimize their performance. In view of this, Bolaji and Abiala (2012) carried out theoretical and experimental analyzes of the behavior of heat transfer in flat-plate absorber solar with water tubes distributed over its entire width. In their work, the performances of the studied system were evaluated and compared both theoretically and experimentally. The ob-

tained results show that the collector efficiency is high especially around mid-day when the collector receives the highest energy and the useful heat rate is at a maximum, also, the collector efficiency increases as the heat rate increases until a maximum value is reached. After, a numerical analysis was used by Ekramian *et al.* (2014) to investigate the effect of different parameters on the thermal efficiency of flat plate solar collectors. Various geometries were examined to assess the influence of geometrical characteristics and operating conditions on the thermal efficiency of solar collectors. In that work, the results obtained show that the thermal efficiency of solar collectors increases with increasing the absorber conductivity, fluid flow rate, plate absorptivity, absorber thickness, and glass transmissivity. Also, the effect of artificial roughness in the form of thin circular wire in V-shaped, multi v-shaped ribs and multi v-shaped ribs with gap geometries on heat transfer and friction factor and performance enhancement of a solar air heater duct are analyzed by Kumar (2014). Here, the author is based on CFD analysis. The found results show that the optimal enhancement in heat transfer and friction factor is observed in the multi v-shaped ribs with a gap as compared to other shapes V-shaped ribs and multi v-shaped ribs roughened solar air heater duct. Later, Jin *et al.* (2015) have investigated numerically the heat transfer and fluid flow in a solar air heater duct with multi V-shaped ribs on the absorber plate. These Chinese researchers found that the multi V-shaped ribs enormously

[†]Corresponding author. Email: elyazid_flihi@yahoo.fr

improved the heat transfer, and the increase in relative rib pitch for the range of parameters investigated, cause to decrease in the average Nusselt number, friction factor, and thermohydraulic performance parameter. Furthermore, a CFD analysis has been carried out by Al-Abbas (2017) to increase the performance of the thermal collectors in multipurpose solar heating systems. In this study, the 3-D computational domain of the solar water heater and the 3-D computational domain of the solar air heater has been used. In the case of multipurpose solar water heating (MPSWH) system, the CFD simulated results have been compared with experimental results examined by Venkatesh and Christraj (2015), and the discrepancies fall within 9.46% in the summer season and 8.31% for the winter season. In the same way for the multipurpose solar air heating (MPSAH) system, the differences between the experimental and numerical results were 6.54% and 10.84% respectively, and it indicates that the found results are within acceptable limits. In the same sense, other researchers have investigated the solar air collectors numerically and experimentally in order to enhance their performance Chabane et al. (2013); Farjallah et al. (2016); Karanth and Cornelio (2017); Menni et al. (2018); Ambarita et al. (2018); Kottayat et al. (2020).

Recently, Ammar et al. (2019) have studied numerically the effects of geometric parameters of baffles on the efficiency of solar air collectors as well as on the behavior of heat transfer and fluid flow within the collector. The results found show that the pressure drop in the air duct also strongly depends on the volume flow, on the other hand, the number of fins has a remarkable effect on the pressure drop. Laaraba (2019) has numerically studied heat transfer in a flat solar thermal collector with partitions attached to its glazing. Here, the author analyzed the effects of the number and length of fins on the air configuration and heat transfer. It found that increasing the number of partitions to the glazing wall leads to a decrease significantly in the value of average Nusselt, and therefore minimization of heat loss to the outside of flat solar thermal collector. Manjunath et al. (2019) evaluated the effect of pin fin array on the instantaneous thermal and effective efficiency of flat plate solar air heater using three dimensional CFD analysis for different flow rate conditions, as well as the influence of fin diameter and longitudinal pitch on the effective efficiency will be brought out. They found that larger fin diameter and lower pitch distances of pin fin produce a relatively higher instantaneous thermal efficiency. On the other hand, increasing the pitch value greater than 40mm for a given diameter does not provide significant gain in terms of effective efficiency. Very recently, Sharma et al. (2020) investigated exergy analysis of nanofluid flow through heat exchanger channels. The net impact of relative variations in the thermophysical properties of the nanoparticles, which were sensitive to numerous parameters including size and shape, material and concentration, as well as based fluid thermal properties, was used to determine the improvement of exergy efficiency of nanofluid flow through heat exchanger. Also, Ibrahim and Kasem (2021) presented a novel thermal study of absorber/receiver circular pipe of parabolic trough solar collector system for laminar and turbulent ($k-\epsilon$ model) fluids flow. In this numerical study, simulations are performed using CFD ANSYS FLUENT software. The obtained results show that the heat transfer coefficient and Nusselt number increase with the increase of the Reynolds number while drag and skin friction coefficients decrease. In addition, the temperature of the thermal output of the parabolic collector at the absorber tube wall increases with rising heat flux, and, it is increased from 350 to 390 K in laminar flow and from 310 to 325 K in a turbulent flow. Kumar et al. (2021) presented a comprehensive review of performance analysis of with and without fins SAH. The authors found that the thermal efficiency increases continuously with an increase in fluid mass flow rate, whereas thermohydraulic efficiency increases up to an inception value of fluid mass flow rate, attains a maximum, and then decreases sharply for a given fin spacing and fin height. Also, considerable work has been done by Rouissi et al. (2021). This study has focused on the effect of baffles and their orientation on the global thermal efficiency of the solar flat air collector. This investigation

is conducted by a CFD numerical parametric study which intended to test the effect of the forms of baffles on the heat transfer inside the air cavity. The results of the CFD simulations showed that the combination of the orientation of 45° with a roughness pitch of $b/a = 2$ increases the SFAC thermal performance, which can reach 85%.

The aim of this work is to study the thermal and dynamic behavior of air flow in a horizontal channel of a flat air solar collector using three geometric shapes of the absorber. This study will be based on a parametric analysis to predict the influence of thermal and design parameters on the energy performance of the collector. The numerical simulations are performed by a CFD code.

2. FORMULATION OF THE PROBLEM

The geometry of the physical problem studied is illustrated in Fig. 1. The computational domain is a rectangular two-dimensional channel of height H and length L . The upper side of the channel is composed of an absorber of length L_u exposed to a constant solar flux density ϕ and an isolated part of length L_e . The insulated bottom face of the channel of length $L = L_e + L_u$, such as the inlet length L_e was chosen to ensure a developed flow at the inlet to the channel. The working heat fluid (air) enters the channel with a mass flow m_p and an inlet temperature T_e and leaves with an outlet temperature of T_s taking into account the heat exchange with the absorber. The dimensions of the channel are shown in Table 1. Note that three forms of the absorbent plate are used, which are presented in Fig.2.

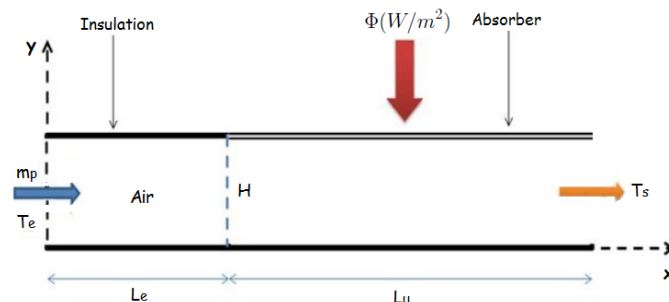


Fig. 1 Physical model and coordinates

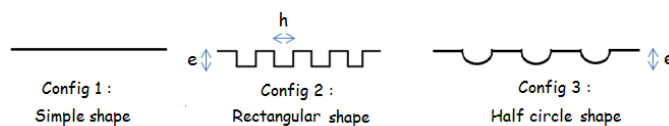


Fig. 2 Absorber configurations

Table 1 Geometric dimensions of the channel.

Portion	size (m)
L	1.6
L_e	0.2
L_u	1.4
H	0.025
h	0.004
e	0.0125

3. SOLAR COLLECTOR MODELING

3.1. Governing equations

In general, The continuity, momentum equations, and energy equation governing the flow and thermal exchanges within the flat solar collector, and which are used by CFD code, are given by the system of equations (1). This numerical contribution is based on the following simplifying assumptions:

- The fluid (water) is Newtonian and incompressible.
- The flow is unsteady, laminar and two-dimensional.
- The viscous dissipation is neglected.
- All properties of the fluid are considered constant except for the density that is assumed to be a function of temperature.
- The Boussinesq approximation is applied.

$$\begin{cases} \frac{\partial \rho}{\partial t} + \nabla(\rho \vec{v}) = 0 \\ \frac{\partial \rho \vec{v}}{\partial t} + \nabla(\rho \vec{v} \vec{v}) = -\nabla p + \nabla \cdot [\mu(\nabla \vec{v} + \nabla \vec{v}^T)] + \rho \vec{g} + \vec{F} \\ \frac{\partial \rho E}{\partial t} + \nabla \cdot [\vec{v}(\rho E + p)] = \nabla \cdot (k_{eff} \nabla T) + S_h \end{cases} \quad (1)$$

3.2. Solving method

A numerical investigation has been made for steady laminar and two-dimensional flow and thermal exchanges within the flat solar collector. The numerical solutions are carried out using Fluent solver based on the finite volume method. For all of our simulations, the mesh of the study domain was done by the automatic mesh generator DesignModeler. The mesh that we adopted for our simulations in the case of simple absorber is presented in Fig.3. Moreover, to ensure the adopted mesh size results independence, several tests were performed For our calculations, and for a compromise between precision and computing time, the grid of 180000 cell is used.

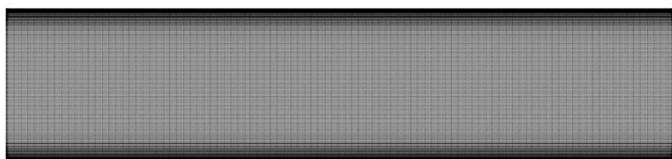


Fig. 3 Mesh adopted by our simulations

3.3. Boundary conditions

In the following diagram, we have summarized all the boundary conditions $\Gamma_i, (i = 1, \dots, 4)$ associated with the problem of convective heat transfer in a flat plate solar collector.

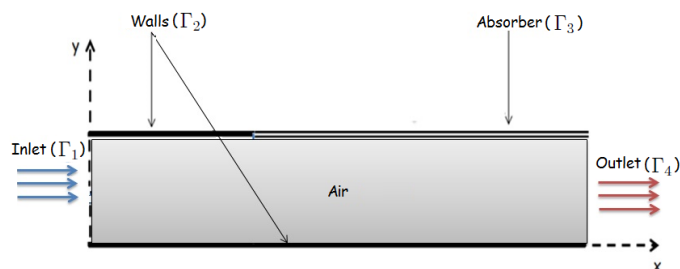


Fig. 4 Tube boundary conditions

Table 2 Boundary conditions used in CFD calculations.

Zone	Zone type	Boundary conditions
Γ_1	Inlet	$m = m_p,$ and $T = T_e$
Γ_2	Walls	$\frac{\partial T}{\partial n} = 0,$ and $u = v = 0$
Γ_3	Absorber	$\phi = cte$ and $u = v = 0$
Γ_4	Outlet	$\frac{\partial T}{\partial n} = \frac{\partial u}{\partial n} = \frac{\partial v}{\partial n} = 0$

3.4. Physical model validation

In order to verify the accuracy of the numerical results obtained in this work by the CFD analysis. A comparison of our numerical results with the literature experimental data of Demartini *et al.* (2004), obtained in the case of the rectangular baffle, in terms of the velocity profiles at the position $x = 0.525 m$ was made and presented in Fig. 5. We can clearly see that this comparison shows a very good agreement between the two results.

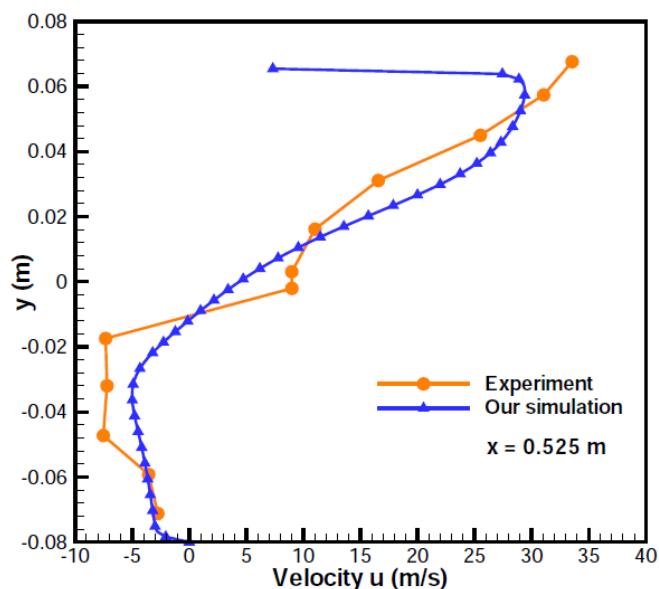


Fig. 5 Comparison of numerical and experimental velocity profiles near the channel outlet

4. SIMULATION RESULTS AND ANALYSIS

4.1. Velocity profiles

Figure 6 shows the effect of the geometric shape of the absorber, at $x = 0.98 m$, on the axial velocity profiles for $m_p = 0.03 kg/s, \phi = 800 w/m^2$ and $T_e = 20^\circ C$. For the first configuration (simple absorber) we notice that the axial speed takes a parabolic shape and reaches its maximum value in the middle of the channel, unlike configurations 2 and 3 where the maximum speeds increase and shift towards the lower part of the channel.

For the last two configurations, the negative speeds observed in the upper part of the channel indicate the presence of a recirculation zone behind the first baffle of the absorber.

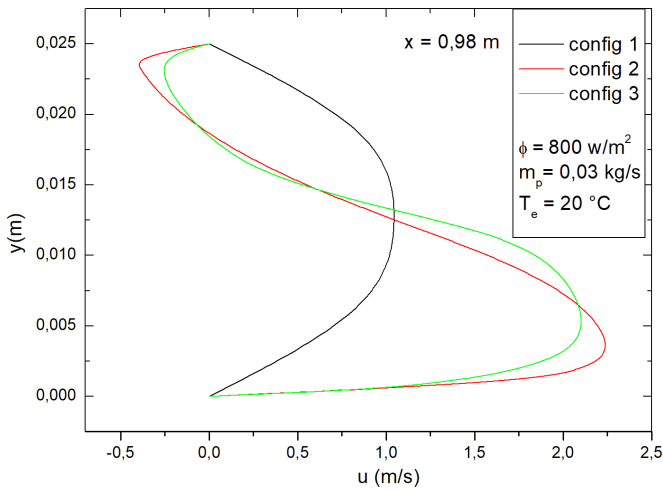


Fig. 6 Axial velocity of the flow in position $x = 0.98m$

4.2. Temperature contours

The effect of the geometric shape of the absorber on the distribution of the thermal field within the channel, for $m_p = 0.03 \text{ kg/s}$, $\phi = 800 \text{ w/m}^2$ and $T_e = 20 \text{ }^\circ\text{C}$ is illustrated in Fig. 7. From this figure, we find that the temperature distribution is homogeneous at the entrance to the channel. On the other hand, at the level of the absorber, the influence of the convective exchange between the absorber plate and the air is more remarkable for the three configurations. In addition, it is noted that the last two forms of the abbreviation allow to further improve the thermal homogeneity at the exit of the channel compared to the first one.

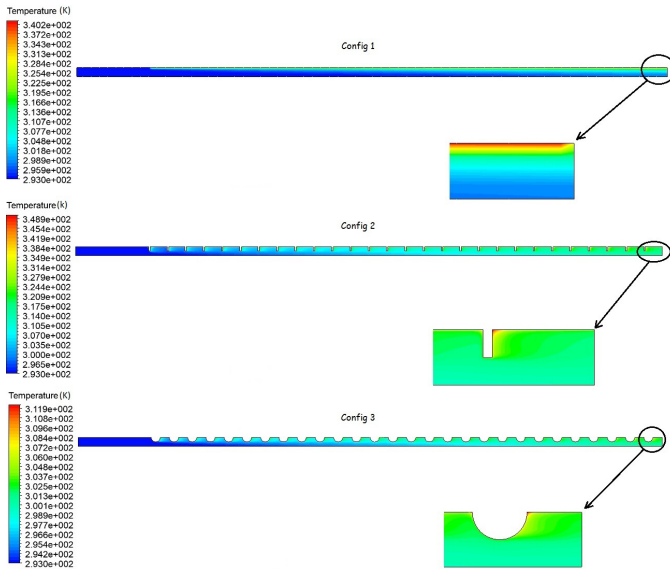


Fig. 7 Temperature distribution within the channel for the three forms of the absorber

4.3. Temperature profiles

Figure 8 shows the effect of the mass flow rate of the air entering the duct on the average outlet temperature for $\phi = 800 \text{ w/m}^2$ and $T_e = 20 \text{ }^\circ\text{C}$. From this figure, it can be seen that the more the mass flow rate increases, the outlet temperature of the heat transfer fluid decreases. On the other hand, the last two configurations make it possible to improve the average outlet temperature compared to the first configuration. Thus, for the mass flow rates less than 0.025 kg/s , it is noted that configuration

3 is the one that gives the best average outlet temperature, beyond this value configuration 2 becomes the best.

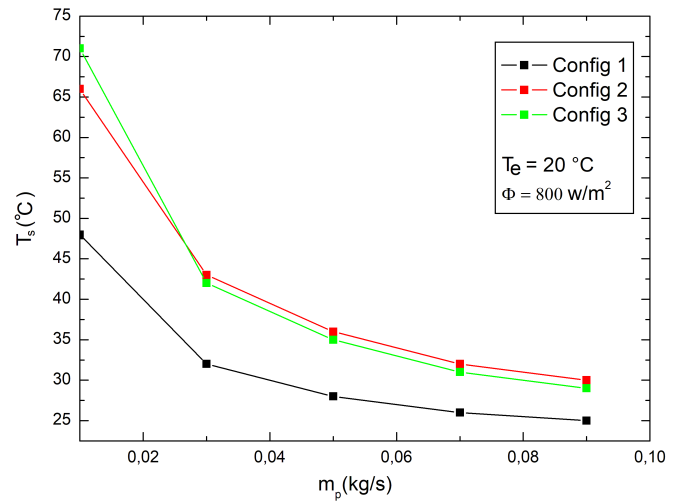


Fig. 8 Effect of mass flow on average temperature profiles at the outlet of the channel

Figure 9 shows the effect of solar irradiation on the air outlet temperature for a mass flow rate of 0.03 kg/s and an inlet temperature of $20 \text{ }^\circ\text{C}$. From this figure, it can be seen that the average air outlet temperature increases linearly with the intensity of the solar flux regardless of the configuration of the absorbent plate. In addition, for a fixed value of solar flux, we see that configuration 2 is the one that gives us the correct air outlet temperature.

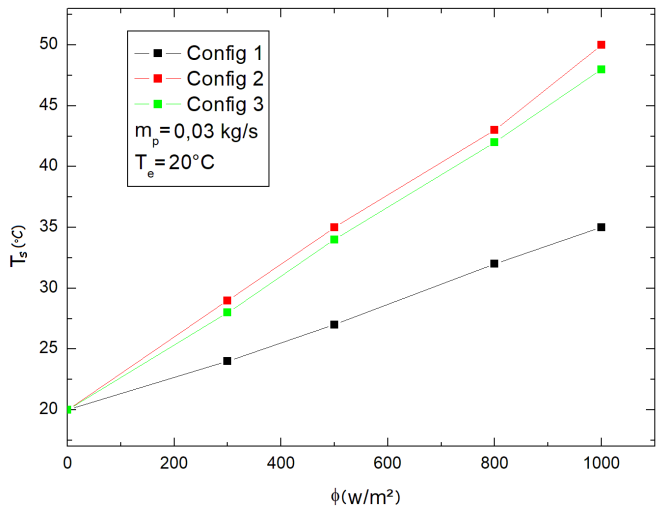


Fig. 9 Effect of ϕ on average temperature profiles at the outlet of the channel for the three configurations

Figure 10 show the effect of the inlet temperature of the heat transfer fluid on the outlet temperature of the air for a mass flow rate of 0.03 kg/s and a mass flow rate of 0.03 kg/s . From this Figure, we deduce that the average air outlet temperature increases linearly with temperature T_e regardless of the absorbent plate shape. On the other hand, we note that the second configuration makes it possible to have a good outlet temperature of the heat transfer fluid regardless of the inlet temperature.

4.4. Nusselt number profiles

Figure 11 shows the effect of the mass flow rate of the air entering the channel on the average Nusselt number at the surface of the absorbent

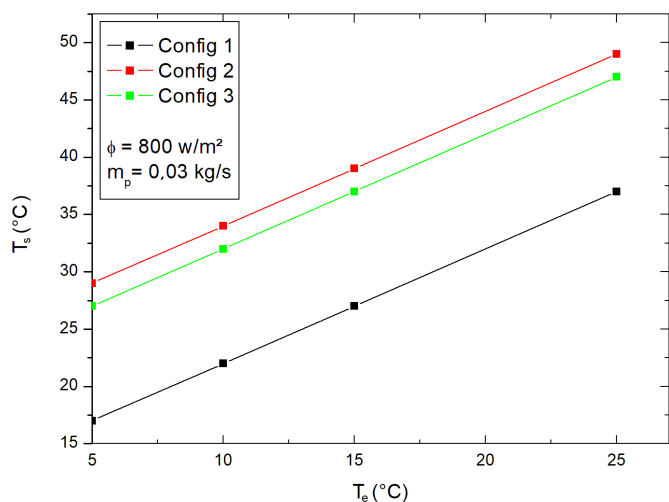


Fig. 10 Average temperature profiles at the outlet of the channel as a function of T_e

plate or $\phi = 800 \text{ w/m}^2$ and $T_e = 20^\circ\text{C}$. From this figure, we deduce that the heat transfer flow rate at the surface of the absorbent plate increases when the mass flow rate increases independently of the geometric configuration of the absorber, and it amplifies more from configuration 1 to configuration 3 regardless of the inlet flow.

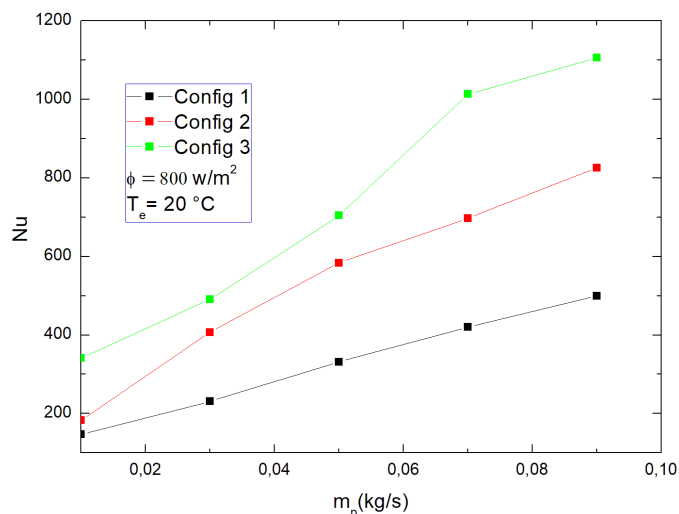


Fig. 11 Effect of mass flow on the mean Nusselt number profiles for the three configurations

Figure 12 shows the effect of solar irradiation on the surface heat transfer rate for a mass flow rate of 0.03 kg/s and an inlet temperature of 20°C . From this figure, we observe that the surface heat transfer rate increases with the intensification of the solar flux for the three configurations of the absorber and it is particularly amplified for configuration 3 in comparison with the other two configurations.

Figure 13 shows the effect of the temperature of the entering fluid (air) on the heat transfer rate at the surface of the absorbent plate for a solar flux equal to 800 W/m^2 and a mass flow rate of 0.03 kg/s . From this figure, it is concluded that the increase in the air inlet temperature leads to a decrease in the rate of heat transfer to the surface of the absorbent plate, for all the configurations studied. In addition, it is noted that configuration 3 makes it possible to have an optimum heat transfer rate compared to the other two configurations.

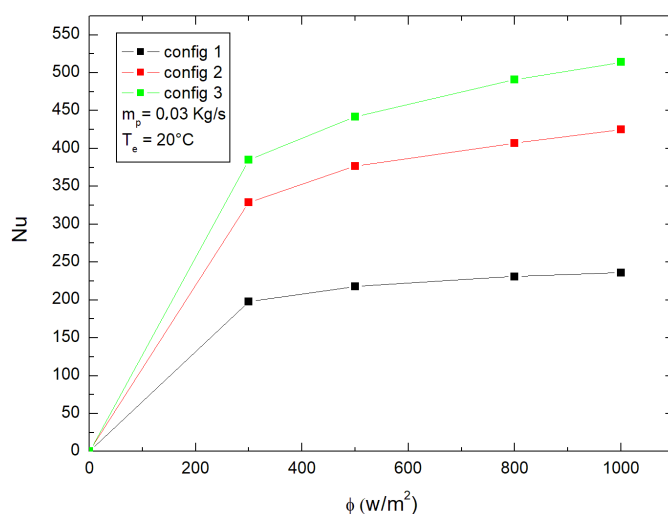


Fig. 12 Effect of ϕ on the mean Nusselt number profiles for the three configurations

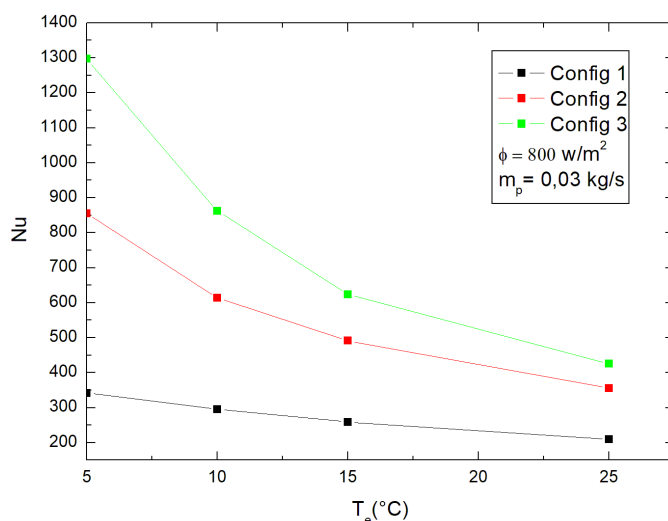


Fig. 13 Mean Nusselt number profiles as a function of T_e for the three configurations

5. CONCLUSIONS

The thermal behavior of the solar air collector with three forms of the absorber plate was numerically investigated. From the present study, the main conclusions are drawn as follows:

- The low mass flow rates of the air increase the average outlet temperature.
- The use of the second configuration of the absorber (rectangular shape) increases the velocity of the air at the downstream of the channel and promotes more thermal homogeneity at the outlet of the channel.
- The average outlet temperature of the air increases linearly with solar flux and inlet temperature.
- For the mass flow rates greater than 0.025 kg/s , the second configuration of the absorber (rectangular shape) is optimal for having a better average air temperature at the outlet of the channel.

NOMENCLATURE

<i>CFD</i>	Computational Fluid Dynamics
<i>e</i>	Baffle height (<i>m</i>)
<i>E</i>	Total energy (<i>J</i>)
<i>F</i>	External body force (<i>N</i>)
<i>g</i>	Gravity acceleration (<i>m/s²</i>)
<i>h</i>	Baffle width (<i>m</i>)
<i>k_{eff}</i>	Effective thermal conductivity (<i>w/m.k</i>)
<i>L</i>	length of conduit (<i>m</i>)
<i>Le</i>	Length of inlet zone (<i>m</i>)
<i>Lu</i>	Length of useful zone (<i>m</i>)
<i>m_p</i>	Mass flow (<i>Kg/s</i>)
<i>p</i>	Pression (<i>pa</i>)
<i>S_h</i>	Heat source term
<i>t</i>	Time (<i>s</i>)
<i>T_e</i>	the fluid inlet temperature (<i>K</i>)
<i>T_s</i>	Mean fluid outlet temperature (<i>K</i>)
<i>u</i>	Velocity in x-direction (<i>m/s</i>)
<i>v</i>	Velocity in y-direction (<i>m/s</i>)
<i>x, y</i>	Cartesian coordinates (<i>m</i>)
<i>Greek Symbols</i>	
<i>ρ</i>	Fluid density (<i>Kg/m³</i>)
<i>φ</i>	Solar flux density (<i>w/m²</i>)
<i>μ</i>	Dynamic viscosity (<i>Pa.s</i>)
<i>Subscripts</i>	
<i>ini</i>	Initial
<i>eff</i>	Effective

REFERENCES

- Al-Abbas, A., 2017, "Computational fluid dynamics (CFD) modeling study of thermal performance for multipurpose solar heating system," *Al-Nahrain Journal for Engineering Sciences (NJES)*, **20**(1), 222–234.
- Ambarita, H., Peranginangin, S.E., Napitupulu, R.A.M., Tampubolon, M., and Sihombing, H.V., 2018, "Numerical simulation of heat transfer of an absorber with fin of a flat-plate type solar collector," *IOP Conf Series: Materials Science and Engineering*, **420**.
- Ammar, M., Mokni, A., Mhiri, H., and Bournot, P., 2019, "Numerical analysis of a flat plate solar collector with baffles in the air duct," *International Journal of Scientific Research & Engineering Technology (IJSET)*, **9**(2), 1–5.
- Bolaji, B.O., and Abiala, I., 2012, "Theoretical and Experimental Analyses of Heat Transfer in a flat plate solar collectors," *Walailak Journal of Science and Technology (WJST)*, **9**(3), 239–248.
<http://dx.doi.org/10.2004/wjst.v9i3.227>.
- Chabane, F., Moumami, N., Brima, A., and Benramache, S., 2013, "Thermal efficiency analysis of a single-flow solar air heater with different mass flow rates in a smooth plate," *Frontiers in Heat and Mass Transfer (FHMT)*, **4**(1).
<http://dx.doi.org/10.5098/hmt.v4.1.3006>.
- Demartini, L., Vielmo, H.A., and Miller, S.V., 2004, "Numeric and experimental analysis of the turbulent flow through a channel with baffle plates," *Journal of the Brazilian Society of Mechanical Sciences and Engineering*, **26**(2).
- Ekrastian, E., Etemad, S.G., and Haghshenasfard, M., 2014, "Numerical analysis of heat transfer performance of flat plate solar collectors," *Journal of Fluid Flow, Heat and Mass Transfer (JFFHMT)*, **1**, 38–42.
<http://dx.doi.org/10.11159/jffhmt.2014.006>.
- Farjallah, R., Chaabane, M., Mhiri, H., Bournot, P., and Dhauoudi, H., 2016, "Thermal performance of the u-tube solar collector using computational fluid dynamics simulation," *J Sol Energy Eng*, **138**(6).
<http://dx.doi.org/10.1115/1.4034517>.
- Ibrahim, M.M., and Kasem, M.M., 2021, "Numerical thermal study of heat transfer enhancement in laminar-turbulent transition flow through absorber pipe of parabolic solar trough collector system," *Frontiers in Heat and Mass Transfer (FHMT)*, **17**(20).
<http://dx.doi.org/10.5098/hmt.17.20>.
- Jin, D., Zhang, M., Wang, P., and Xu, S., 2015, "Numerical investigation of heat transfer and fluid flow in a solar air heater duct with multi V-shaped ribs on the absorber plate," *Energy*, **89**, 178–190.
<http://dx.doi.org/10.1016/j.energy.2015.07.069>.
- Karant, K.V., and Cornelio, J.A.Q., 2017, "CFD Analysis of a flat plate solar collector for improvement in thermal performance with geometric treatment of absorber tube," *International Journal of Applied Engineering Research*, **12**(14), 4415–4421.
- Kottayat, N., Kumar, S., Yadav, A.K., and Anish, S., 2020, "Influence of rectangular ribs on exergetic performance in a triangular duct solar air heater," *J Thermal Sci Eng Appl*, **12**(5).
<http://dx.doi.org/10.1115/1.4046057>.
- Kumar, A., 2014, "Analysis of heat transfer and fluid flow in different shaped roughness elements on the absorber plate solar air heater duct," *Energy Procedia*, **57**, 2102–2111.
<http://dx.doi.org/10.1016/j.egypro.2014.10.176>.
- Kumar, S., Thakur, R., Suri, A.R.S., Kashyap, K., Singhy, A., Kumar, S., and Kumar, A., 2021, "A comprehensive review of performance analysis of with and without fins solar thermal collector," *Frontiers in Heat and Mass Transfer (FHMT)*, **16**(4).
<http://dx.doi.org/10.5098/hmt.16.4>.
- Laaraba, A., 2019, "Numerical study of heat transfer in a flat plate thermal solar collector with partitions attached to its glazing," *Thermal Science*, **23**(2B), 1075–1084.
<http://dx.doi.org/10.2298/TSCI170531101L>.
- Manjunath, M.S., Karant, K.V., and Yagnesh, S.N., 2019, "Numerical analysis of flat plate solar air heater integrated with an array of pin fins on absorber plate for enhancement in thermal performance," *J Sol Energy Eng*, **141**(5).
<http://dx.doi.org/10.1115/1.4043517>.
- Menni, Y., Azzi, A., and Chamkha, A., 2018, "A review of solar energy collectors: Models and applications," *Journal of Applied and Computational Mechanics*, **4**, 375–401.
<http://dx.doi.org/10.22055/JACM.2018.25686.1286>.
- Rouissi, W., Naili, N., Jarray, M., and Hazami, M., 2021, "CFD Numerical investigation of a new solar flat air-collector having different obstacles with various configurations and arrangements," *Mathematical Problems in Engineering*, **2021**, 1–7.
<http://dx.doi.org/10.1155/2021/9991808>.
- Sharma, L., Kumar, S., Thakur, R., Goel, B., Suri, A.R.S., Thapa, S., Kumar, N., Maithani, R., and Kumar, A., 2020, "A review on exergy analysis of nanofluid flow through several conduits," *Frontiers in Heat and Mass Transfer (FHMT)*, **14**(30).
<http://dx.doi.org/10.5098/hmt.14.30>.
- Venkatesh, R., and Christraj, W., 2015, "Experimental investigation of multipurpose solar heating system," *Journal of Energy engineering*, **141**(3).
[http://dx.doi.org/10.1061/\(ASCE\)EY.1943-7897.0000166](http://dx.doi.org/10.1061/(ASCE)EY.1943-7897.0000166).